Study of coupled heat and water transfer in proton exchange membrane fuel cells by the way of internal measurements

A Thomas, G Maranzana, S Didierjean, J Dillet and O Lottin

LEMTA, University of Lorraine, 2 Avenue de la Forêt de Haye, BP 160, 54504 Vandoeuvre-lès-Nancy Cedex, France

Email : anthony.thomas@univ-lorraine.fr

Abstract. Measurements of electrode temperatures within a proton exchange membrane fuel cell were performed using platinum wires. A temperature difference of 7°C between the electrodes and the bipolar plates was observed for a cell operating at a current density of 1.5 A.cm^{-2}. These measurements show a strong non-uniformity of the temperature profile through membrane electrode assembly (MEA) that future phenomenological models must take into account. In addition, the simultaneous measurements of heat and water flux through the MEA leads to the conclusion that produced water crosses the diffusion layer in vapor phase. A very simple heat transfer model is proposed.

Nomenclature

F	Faraday constant $C.mol^{-1}$
RH	relative humidity
T	temperature $°C$
U	voltage V
I	current intensity A
j	current density $A.cm^{-2}$
N	water flux $mol.s^{-1}$
LHV	lower heating value $kJ.mol^{-1}$
HHV	higher heating value $kJ.mol^{-1}$
Lv	latent heat of water $kJ.mol^{-1}$
e_{GDL}	porous layer thickness μm
R	thermal resistance of the porous layer $K.W^{-1}$

Greek symbol	
Φ	Heat flux W
λ	conductivity $W.m^{-1}.K^{-1}$
Subscripts and superscripts	
a	anode
c	cathode
$cond$	conductive
e	electrode
i	inferior
s	superior
th	theoretical

1. Introduction

Proton exchange membrane fuel cells (PEMFC) make it possible to convert efficiently chemical energy into electrical energy. Using hydrogen as fuel, they can produce electricity over a wide range of power without on-site emission of greenhouse gases, the only reaction product being water. PEMFC is currently used for powering electric vehicles, portable electronic applications and cogeneration of small and medium power. They operate at nominal temperatures low enough (60 to 90 °C) and start at room temperature.

Despite recent technological advances, their large-scale commercialization is still hampered by issues of cost (platinum catalyst and polymer membrane prices) and durability that can be related to water management within the cell (electrode corrosion, dissolution of platinum, oxygen transport). The study of water transport in a proton exchange membrane fuel cell is therefore fundamental.

50% to 70% of the energy exiting the cell as heat, recent works have therefore examined the impact of the temperature field on water transport in the fuel cells MEA [1-10]. In 2002, Djilali and Lu [1] focused on the modeling of non-isothermal and non-isobaric effects (including Knudsen diffusion and Soret effects). They found a typical mean temperature difference of 1 to 5°C, between the bipolar plate and the cathode, function of the current density and thermo-physical properties of materials. Weber and Newman [2] and Wang and Wang [3] showed, by considering a non-isothermal operation of the fuel cell, that evaporation/condensation (heat pipe effect) through the porous layer may have a significant effect at high current densities. Eikerling [4] also showed that at a current density of 1 $A.cm^{-2}$, the evaporation rate at the electrode is sufficient to remove all water produced at the cathode in vapor phase. To visualize this phenomenon, Hickner et al. [5,6], Kim and Mench [7,8] and Fu et al. [9], used neutron radiography highlighted the importance of evaporation at high current densities. The temperature influence on the water is significant, on its state but also on its transport. Indeed, the works of Kim and Mench, Fu et al. or Hatzell et al. [10] showed that water goes preferentially towards the colder side of the fuel cell. Because of this phenomenon, it is important to realize accurate measurements of temperature in all parts of the cell.

Temperature measurements within an operating fuel cell have been already performed. In 2004, Vie and Kjelstrup [11] were the first to measure the local temperature near the electrodes using thermocouples (120 μm in diameter). By measuring the temperature at the membrane/electrode interface and channel/GDL interface, they calculated the thermal conductivity of the membrane and of the electrode+GDL. Zhang et al. [12,13] used thermocouples with a diameter of 100 μm that they placed at the GDL/electrode interface to measure the temperature difference between the air flow at the inlet and at the outlet of the cathode compartment. They observed a correlation between the local temperature and the local current density. A difference of 5°C was measured between the electrode and the bipolar plate for a current density of 1 $A.cm^{-2}$. A correlation between local temperature, current density and the presence of liquid water was also put forward by Maranzana et al. [14] using a segmented and transparent fuel cell; the temperature measurement was done using thermocouples inserted along the air channels.

To complete these studies, an experimental approach is developed in this work. It consists in measuring internal temperatures in a proton exchange membrane fuel cell, using small platinum wires which diameters are more adapted to the electrode thickness than thermocouples. Beside, heat and water fluxes are measured on the anode and cathode sides. These measurements allow confirming - at least for our operating conditions - that produced water crosses the diffusion layer in vapor phase. In addition, the effective thermal conductivity of porous layers, a key parameter for the analysis of heat transfer in the fuel cell is estimated in situ.

2. Experimental set up

A hydrogen fuel cell is a cell in which the electrical power generation is obtained by hydrogen oxidation at the anode and oxygen reduction at the cathode. For this, a membrane electrode assembly (MEA) is sandwich between porous layers (to obtain a homogeneous diffusion of gases over the entire surface of electrodes) and bipolar plates which ensure the supply of hydrogen and air.

The MEA considered for this experiment was purchased from Johnson Matthey Technology. It consists of a 30 μm perfluorosulfonated membrane and two 10μm thick electrodes with a platinum loading of 0.2 $mg.cm^{-2}$ at the anode and 0.6 $mg.cm^{-2}$ at the cathode. The square surface of the MEA is 25 cm^2. Hydrogen and air flow in plates consisting of 28 parallel channels of 50 mm in length, 1 mm in width and 0.4 mm in depth. The porous layers, placed between the plates and the active layers, are developed by Sigracet ® and consist of a 375 μm thick porous medium made of carbon fibers coated

with 5% PTFE called GDL (Gas Distribution Layer), and a 45µm thick microporous medium (MPL) strongly hydrophobic (30% PTFE).

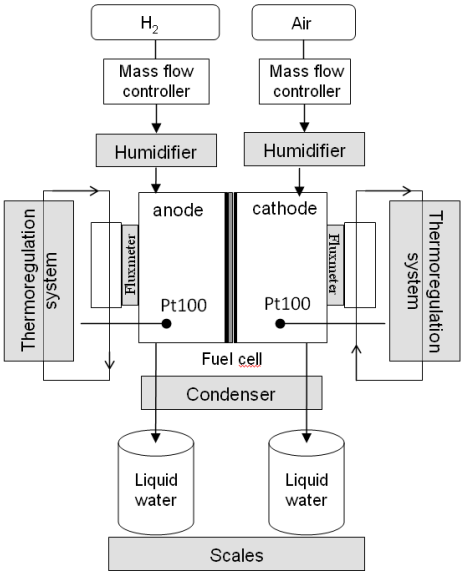

Figure 1. Scheme of the experimental setup

The scheme of the experimental setup is shown in figure 1. At the inlet of the cell, hydrogen and air are preheated and humidified using bubblers whose temperature are kept constant equal to 60°C. At the outlet, the gases pass through a condenser maintained at 8°C using a Peltier module. The condensed water is weighed using scales with an accuracy of 0.01g. The water balance between the input and the output of the cell is used to calculate the water flux through the porous layers and the membrane. Simultaneously, the heat flux through the cell is measured using two heat flux sensors placed between thermoregulated aluminum plates and the flow field plates. The temperature of the plates is measured with a platinum probe (Pt100) that controls the temperature of the water that flows through the aluminum plates. The tangential gradient heat flux sensors used are developed by Captec ®. For measuring the temperature of the electrodes, 8 platinum wires are inserted at the electrode/MPL interface (see figure 2).

The Pt wires diameter is 25 µm plus a 5 µm Kapton coating. Thus, the total diameter of wire is 35 µm that is 2-3 times larger than the average diameter of carbon fibers which constitute the GDL.

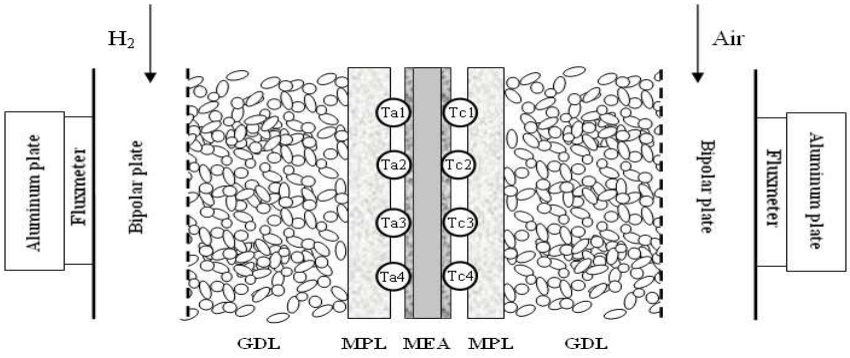

Figure 2. Position of the 8 wires at the electrode/MPL interface. Gases flow from top to bottom.

Wires allow measuring the average temperature along the MEA in the direction perpendicular to the flow. They are manually spaced 1cm out from each other. Consequently, we measure the average temperature perpendicularly to the gas flow or in other words, locally along the gas flow direction.

3. Measurement protocol

3.1. Temperature measurement protocol

The temperature measurement is based on the dependence of the electrical resistance of the platinum wires with the temperature. To obtain the resistance of each wire, a calibration is performed. This operation consists in setting bipolar plate temperatures at the same values, varying between 57°C and 63°C (passing four times by 60°C) without fuel cell operates. Figure 3 shows the variation of the wires voltage (a direct current of 25 mA is set within wires) during the calibration. This calibration allow, by

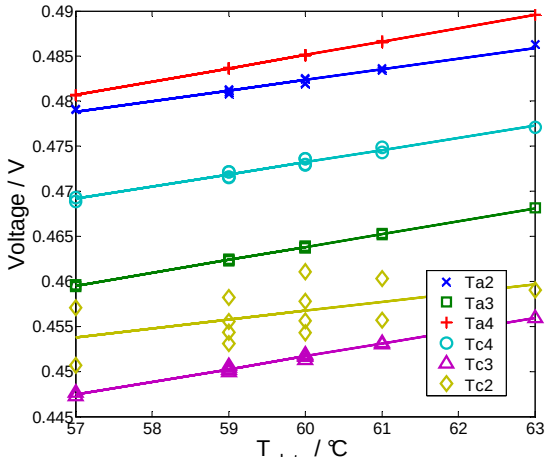

Figure 3. Scheme of the experimental setup

measuring the voltage of each wire during operating fuel cell, to obtain the average temperature along each wire.

The voltage of 6 of the 8 platinum wires as a function of the plates temperature are shown on figure 3. Two wires (*Ta1* and *Tc1*) have been broken during the compression and/or the setting plate temperature (their very small size makes them very fragile). The voltage varies linearly with the temperature and the reproducibility of the measurement is good for 5 wires (*Ta2 Ta3 Ta4 Tc3* and *Tc4*). The intrusiveness of the measurement technique was verified, no change on the performance of the fuel cell or the water fluxes measurements were noted.

3.2. Heat flux measurement protocol

Tangential gradient heat flux sensors deliver a voltage proportional to the incident heat flux. After a calibration stage, the proportionality coefficient, called the sensor sensitivity, was found to be equal to 27.8±3% µV/(W/m²) at the anode side and 23.2±3% µV/(W/m²) at the cathode side. The surface of the sensors is equal to 36 cm^2. To obtain the heat flux through the porous layers, corrections are made on the raw flux measurements. These corrections take into account the heat flux lost due to the imperfect insulation (about 1W per plate measured when I = 0A), the heat flux given by the feeding gases that are overheated after the bubblers (calculated from gases flow and overheat temperatures) and the heat flux associated with water condensation due to the consumption of the gases. When hydrogen and oxygen are consumed, water vapor that saturates these two gases condenses and thus yields a heat flux that should be subtracted to find again the thermodynamics prediction.

4. Results and discussion

All measurements presented below were performed with a stoichiometry of 1.4 for hydrogen and 3 for air. Results are given for a current densities range of 0.04 to 1.5 $A.cm^{-2}$. Three thermal configurations are studied:

- plates temperatures (*Ta* for the anode and *Tc* for the cathode) are equal to 60°C.
- temperature of the cathode plate is set to 62.5°C and the anode to 57.5°C.
- temperature of the anode plate is set to 62.5°C, and the cathode to 57.5°C.

As bubblers temperature is kept constant equal to 60°C, when $Tc = Ta$, relative humidities at the anode (RH_a) and at the cathode (RH_c) are equal to 100%. When $Tc > Ta$, at the inlet RH_a = 89% and RH_c = 100% and inversely, when $Ta > Tc$, RH_a = 100% and RH_c = 89%. Thermal configurations were selected to keep a constant average temperature of 60 °C.

4.1. Electrodes temperature measurement

Temperatures measured at the electrodes are shown in figure 4. The drawings show the temperature rise at the anode and cathode for three current densities, 0.04, 0.8 and 1.5 $A.cm^{-2}$ and three thermal set-ups for the bipolar plates. For each electrode, the temperature values are the average of those measured by each wire.

For the three setups, there is an electrode temperature rise of 7°C for a current density j equal to 1.5 $A.cm^{-2}$, corresponding to a temperature gradient of about 20°C.mm^{-1}. The same temperature increase was observed by Weber and Hickner [15] in the case of equal bipolar plates temperatures. They

measured an electrode temperature 6°C higher than the plate temperature at j = 1.25 A.cm^{-2} for equivalent membrane and porous layers thicknesses.

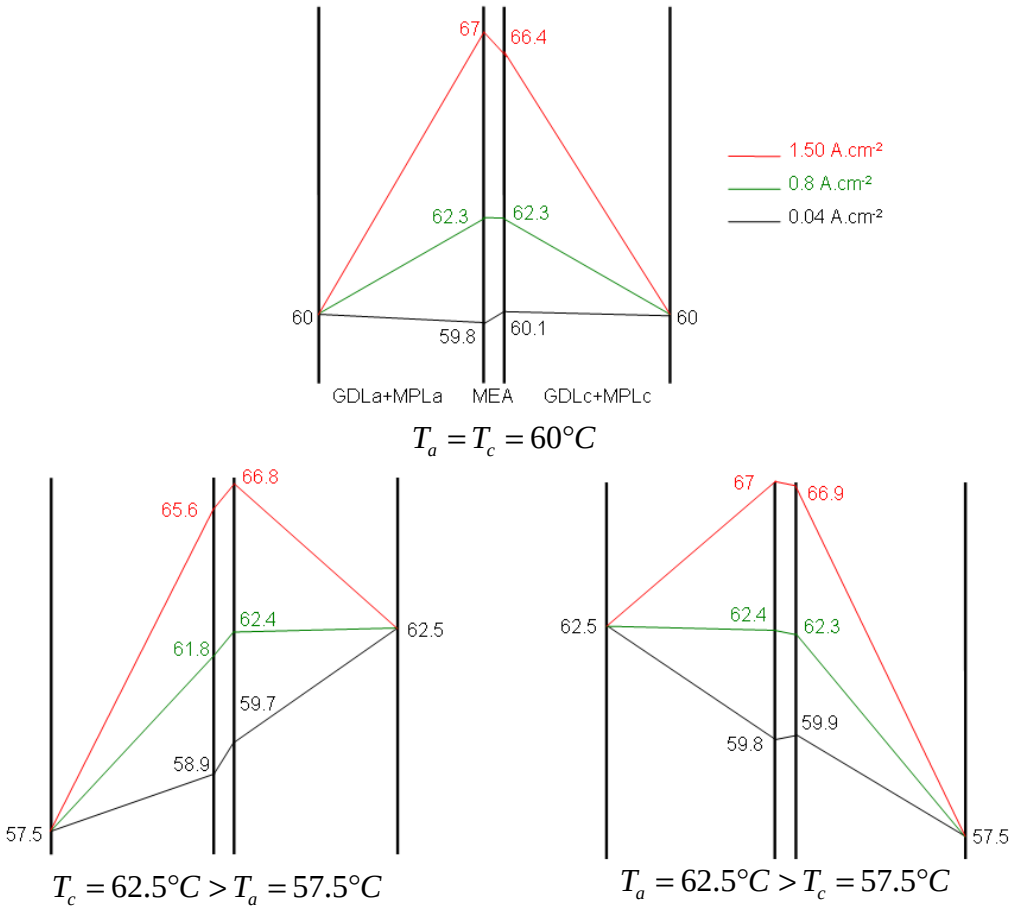

Figure 4. Electrode temperature (°C) vs. current density

A reversal of temperature gradient is observed for j = 1.5 A.cm^{-2} when the plates have a different temperature (*Tc* > *Ta* and *Ta* > *Tc*). A difference of 5°C between *Ta* and *Tc* is not sufficient to obtain a heat flux directed from the hottest plate to the coldest over the entire range of current densities. Moreover, one can notice that the MEA temperature is almost uniform. These measurements show a strong non-uniformity of temperature within the cell. Considering the cell as an isothermal system is not justified.

4.2. Heat fluxes through the porous layers measurement

In the case *Ta* = *Tc*, figure 5.a shows heat fluxes through the porous layers, ϕ_a in blue at the anode side and ϕ_c in green at the cathode side, as a function of the current density. Figure 5.b shows ϕ_a and ϕ_c minus the condensation heat of the water flowing from the electrode to the. $\phi_a^{cond} = \phi_a - N_a Lv$ and $\phi_c^{cond} = \phi_c - N_c Lv$, where water fluxes N_a and N_c were obtained thanks to a mass balance [16].

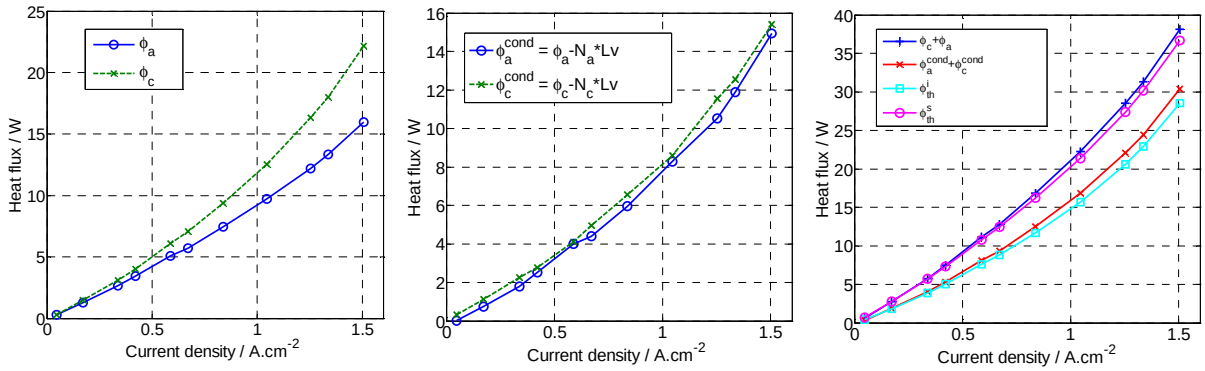

(a) (b) (c)

Figure 5. Heat fluxes measurements on the anode side (ϕ_a) and cathode side (ϕ_c), minus heat of water condensation (b) and comparison with theoretical sources (c) vs. current density. By convention, heat fluxes are considered positive when they are directed from the source (MEA) to the outside. Thermal case *Ta* = *Tc*.

This quantity ϕ^{cond} can be interpreted as the heat transfer by conduction through the porous layers in the case where water crosses the layer in vapor phase without thermal interaction with it. To validate these measures, the total heat flux ($\phi_a + \phi_c$) is compared, on figure 5.c, with the theoretical heat source corresponding to the difference between the total power supplied by the combustion of hydrogen and electrical power given by *UI*:

$$\phi_{th}^{i} = LHV\frac{I}{2F} - UI \quad \text{and} \quad \phi_{th}^{s} = HHV\frac{I}{2F} - UI$$

LHV is the lower heating value (240 kJ.mol^{-1}) and *HHV* the higher heating value (284 kJ.mol^{-1}).

It must be noted that $\phi_a + \phi_c$ is very close to ϕ_{th}^{s}. This validates the heat fluxes corrections and measurements, and provides information that water is in liquid form caused by the condensation on the coldest part of the cell. Figure 5.c also shows that $\phi_a^{cond} + \phi_c^{cond}$ is close to ϕ_{th}^{i}. This indicates that water measurements are accurate and water transport within the porous layers can be therefore in vapor phase.

Of course, an increase of heat fluxes with the current density is observed because the entropic heat of reactions, and irreversibilities (kinetic overpotential and ohmic losses) increase with the current density. When T_c=T_a, heat obtained at the cathode ϕ_c is larger than at the anode ϕ_a (figure 5.a). However, if the heat corresponding to water condensation is subtracted (figure 5.b), it is very interesting to observe that the so amended heat fluxes, ϕ_a^{cond} and ϕ_c^{cond}, are the same at the anode and cathode sides whatever the current density. It is supposed that ϕ_a^{cond} and ϕ_c^{cond} are conductive heat fluxes through the gas distribution layers. They would be the same for both sides because materials and thermal gradients are the same. Thus, heat transfer through the diffusive layer appears as a conductive heat transfer through the GDLs in parallel with phase change heat flux as shown in figure 6.

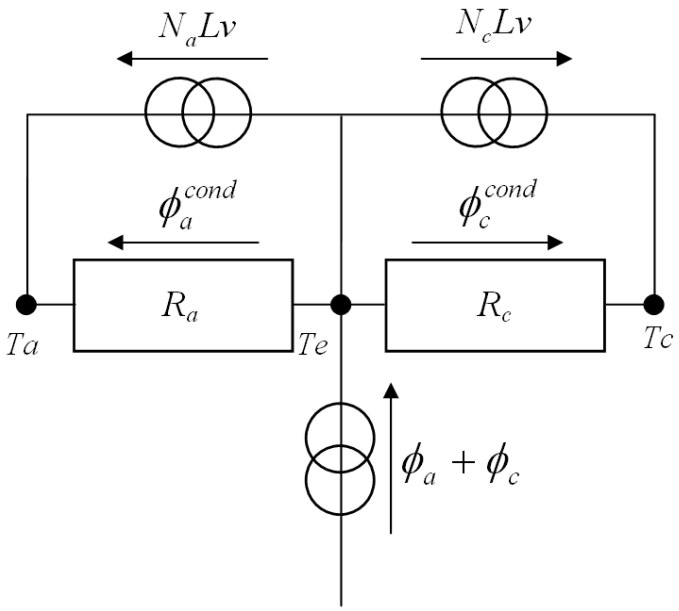

Figure 6. Thermal model of the cell

To confirm this assumption, heat fluxes as functions of the temperature difference between the electrode (*Te*)and the plate facing it (*Ta* or *Tc*), for the three thermal cases (*Ta* = *Tc* = 60°C, *Tc* = 62.5°C > *Ta* = 57.5°C and *Ta* = 62.5°C > *Tc* = 57.5°C) are plotted on the figure 7.

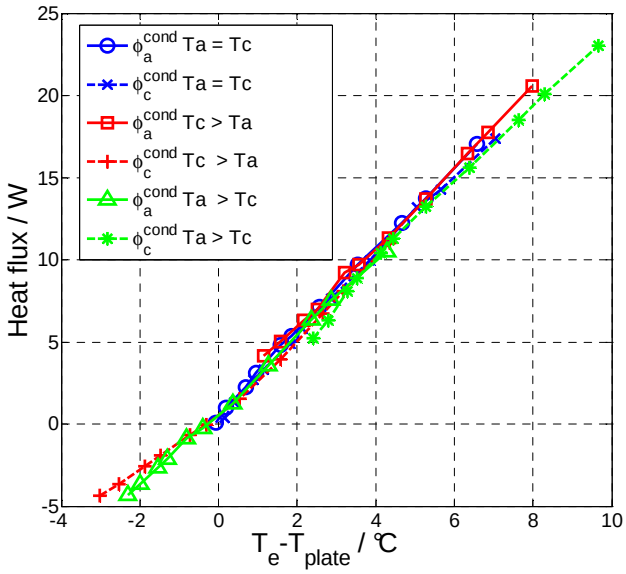

Figure 7. ϕ_a^{cond} and ϕ_c^{cond} as a function of the measured temperature difference between the electrode and the plate facing it for the three thermal cases.

The linearity of heat flux as a function of the temperature difference is a signature of conductive heat transfer. Thus one can estimate the equivalent thermal resistance to the porous layers:

$$R = R_{a,c} = \frac{T_e - T_{a,c}}{\phi_{a,c}^{cond}} = 0.45\ K.W^{-1}$$

This measurement is performed in situ and so includes the contact resistances between the porous layer and the plate. An equivalent thermal conductivity can be derived too:

$$\lambda = \frac{e_{GDL}}{RS} = 0.3\,W.m^{-1}.K^{-1}$$

The same order of magnitude has been found by Ramousse et al. [17] using a standard ex situ hot plate method. Note that in our case, this effective thermal conductivity take the contact and constriction resistances into account.

5. Conclusion

Temperature measurements in the heart of a fuel cell were performed using platinum wires inserted at the electrode/MPL interface. Three thermal configurations with different flow field plate temperatures were examined. A temperature rise of 7°C between the electrodes and the plates was observed for a current density of 1.5 A.cm^{-2}, demonstrating the existence of strong temperature gradients through a cell in operation.

Concomitant measurements of water and heat fluxes allowed asserting and validating, whatever the plates temperatures, a simple thermal model that consider a conductive heat transfer through the porous layers in parallel with a phase change heat transfer driven by the water vapor flow through the pores. The only thermal parameter of this model is the effective thermal conductivity which has been estimated in situ to 0.3W.m^{-1}.K^{-1}. To close this problem, a coupled mass transfer model has to be developed in order to explain the water fluxes and the water sharing between the anode and cathode.

References

[1] Djilali N and Lu D 2002 *Int. J. Therm. Sci.* **41** 29-40
[2] Weber A Z, Newman J 2006 *J. Electrochem. Soc.* **153** A2205-A2214
[3] Wang Y and Wang C Y 2006 *J. Electrochem. Soc.***153** A1193-A1200
[4] Eikerling M 2006 *J. Electrochem. Soc.***153** E58-E70
[5] Hickner M A, Siegel N P, Chen K S, Hussey D S, Jacobson D L and Arif M 2008 *J. Electrochem. Soc.***155** B294-B302
[6] Hickner M A, Siegel N P, Chen K S, Hussey D S, Jacobson D L and Arif M 2008 *J. Electrochem. Soc.***155** B427-B434
[7] Kim S and Mench M M 2009 *J. Electrochem. Soc.***156** B353-B362
[8] Kim S and Mench M M 2009 *J. Membr. Sci.* **328** 113-120
[9] Fu R S, Preston J S, Pasaogullari U, Shiomi T, Miyazaki S, Tabuchi Y, Hussey D S and Jacobson D L 2011 *J. Electrochem. Soc.***158** B303-B312
[10] Hatzell M C, Turhan A, Kim S, Hussey D S, Jacobson D L and Mench M M 2011 *J. Electrochem. Soc.***158** B717-B726.
[11] Vie P J S and Kjelstrup S 2004 *Electrochim. Acta* **49** 1069–1077
[12] Zhang G, Guo L, Ma L and Liu H 2010 *J. Power Sources* **195** 3597-3604.
[13] Zhang G, Shen S, Guo L and Liu H 2012 *Int. J. Hydrogen Energy* **37** 1884-1892
[14] Maranzana G, Lottin O, Colinart T, Chupin S and Didierjean S 2008 *J. Power Sources* **180** 748-754
[15] Weber A Z and Hickner M A 2008 *Electrochim. Acta* **53** 7668-7674
[16] Thomas A, Maranzana G, Didierjean S, Dillet J and Lottin O 2012 *Fuel Cells* **12** 212-224
[17] Ramousse J, Didierjean S, Lottin O, Maillet D 2008 *Int. J. Therm. Sci.* **47** 1-6